Application of Structural Load Feedback in Flight Control

Susan A. Frost[1]
NASA Ames Research Center, Moffett Field, CA, 94035

Khanh V. Trinh[2]
SGT, Moffett Field, CA 94035

Brian R. Taylor[3], Christine V. Jutte[4], John J. Burken[5]
NASA Dryden Flight Research Center, Edwards, CA, 93523

and

Marc Bodson[6]
University of Utah, Salt Lake City, UT 84112

Advances in sensors and avionics computation power suggest real-time structural load measurements could be used in flight control systems for improved safety and performance. A convention transport flight control system determines the moments necessary to meet the pilot's command, while rejecting disturbances and maintaining stability of the aircraft. Control allocation is the problem of converting these desired moments into control effector commands. In this paper, a framework is proposed to incorporate real-time structural load feedback and structural load constraints in the control allocator. Constrained optimal control allocation can be used to achieve desired moments without exceeding specified limits on monitored load points. Furthermore, certain criteria can be minimized, such as loads on certain parts of the aircraft. Flight safety issues could be addressed by using system health monitoring information to change control allocation constraints during flight. The framework to incorporate structural loads in the flight control system and an optimal control allocation algorithm will be described and then demonstrated on a nonlinear simulation of a generic transport aircraft with flight dynamics and static structural loads.

I. Introduction

Reducing the environmental impact of civil aviation and increasing safety is a goal of the NASA Aeronautics Research Directorate[1]. NASA, industry, universities, and other government organizations are researching advanced technologies and exploring novel civil transport configurations to achieve these goals. Environmental impact of aviation, in the form of fuel burn and emissions, will be addressed, in part, by decreasing the weight of aircraft. Advanced materials and reduced structural material decreases the empty vehicle weight, but this comes with challenges created by increased airframe flexibility and vulnerability to exceedance loads. Safe operation of these new vehicles is an important area of research.

The Aviation Safety Program (AvSafe) under the Aeronautics Research Mission Directorate (ARMD) at NASA is working to realize the full potential of the Next Generation Aircraft Transportation System (NextGen). Working with partners, AvSafe provides fundamental research on existing safety challenges and on new and emerging challenges created by the transition to NextGen. Under the umbrella of NASA's Aviation Safety Program, the System-wide Safety Assurance Technologies (SSAT) Project provides knowledge, concepts, and methods to

[1] Computer Engineer, Intelligent Systems Division, M/S 269-3, AIAA Member.
[2] Research Scientist, NASA Ames Research Center, M/S 269-3.
[3] Aerospace Engineer, Controls and Dynamics Branch, PO Box 273, M/S 4840D.
[4] Aerospace Engineer, Aerostructures Branch, PO Box 273, M/S 4820-2A, ASME Member.
[5] Aerospace Engineer, Controls Branch, PO Box 273, M/S 4840D, AIAA Senior Member.
[6] Professor, Electrical and Computer Engineering, 50 S Central Campus Dr. Rm. 3280, AIAA Senior Member.

proactively manage increasing complexity in the design and operation of vehicles and air transportation systems, including prognostic algorithm design and the intersection of flight control with system health management.

System health monitoring provides useful information on the current state of a system that can be used to improve many of its operational objectives[2]. Growing demand for improving the reliability and survivability of safety-critical aerospace systems has led to the development of prognostics and health management (PHM) and fault-tolerant control (FTC) systems. Active FTC techniques that are capable of retaining acceptable performance in the presence of faults are being developed for both inhabited and uninhabited air vehicles[3-5] and researchers are exploring new paradigms and approaches for integrating PHM with controls[6,7]. Typically, a decision-making component reasons over the system health and the objectives and constraints of the system. For instance, a component could be identified as having a fault that would eventually lead to component failure and system shutdown. Decision making using prognostic information on the estimated remaining useful life (RUL) of the component along with operational objectives and constraints may result in changes to the operational mode of the system or to the system's controller. For example, the PHM system might predict an impending actuator fault that would freeze the actuator at its current position. This could have many negative consequences from increased drag, and therefore, greater fuel burn, to issues with aircraft landing. Thus it may be desirable to limit the allowed deflection of the control surface.

Conventional aircraft have a flight control system that follows the pilot's commands, while maintaining stability of the aircraft and rejecting disturbances such as gusts. The flight control system determines the three angular rates in the aircraft body axis that will achieve the desired objectives. Control allocation is the problem of determining aircraft control surface deflections to achieve desired rates. Conventional control allocation schemes control the three angular rates primarily with three control variables. Control allocation on NextGen aircraft will control these rates using a variety of redundant and multi-objective control surfaces. We say a vehicle is *over-actuated* if it has more control effectors than control variables. The control allocation of over-actuated vehicles has been formulated as a constrained optimization problem by many researchers[8-17]. A real-time solution to the control allocation problem is desirable to enable the system to run on NextGen aircraft during flight. This has prompted the search for numerical optimization methods that have good convergence properties and acceptable computational requirements.

We propose a framework to enable a flight control system with optimal control allocation to incorporate real-time structural load feedback and structural load constraints in addition to effector position constraints. Depending on the health of the aircraft, the constraints could be modified. For example, if the PHM system determines that an actuator is likely to get frozen at a non-zero position, the actuator's position limits could be reduced, assuming there was enough control authority to achieve desired commands. A structural health monitoring system might detect a serious structural fault that could potentially affect aircraft safety if it progressed. Structural loads at relevant locations on the aircraft could be minimized as much as possible using the proposed algorithm.

An optimal control allocation algorithm that incorporates structural load measurements with load and actuator constraints will be described and demonstrated on an illustrative example. The proposed framework and control allocation algorithm are evaluated in a simulation of a generic transport aircraft coupled with a structural model of the aircraft to simulate real-time structural loads. The coupled model is used to estimate structural loads on the aircraft during flight and to predict loads generated by control surface deflections. The simulation demonstrates how optimal control allocation with load feedback and system health management information could be used to mitigate safety issues in aircraft.

II. Control Allocation

Several methods to solve the control allocation problem have been evaluated, including direct allocation, linear programming, quadratic programming, and mixed optimization approaches[8-17]. There are advantages and disadvantages to all of the approaches. Control allocation research has also extended the control solution to include coupling or interaction effects between control effectors, creating a nonlinear optimization problem that can often be transformed into a sequence of linear problems[16]. While the interaction effects will be important to study for control allocation in next generation aircraft, this paper will focus on solutions that assume a linear relationship between the effectors and the moments they generate.

A. Control allocation in model reference control

We introduce control allocation in the context of model reference control (a form of dynamic inversion). However, solutions may be used in a variety of control design methods. To state the problem mathematically, we consider the state-space model

$$\begin{aligned} \dot{x}_A &= A_A x_A + Bu + d \\ y_A &= Cx_A \end{aligned} \tag{1}$$

where $x_A \in R^n$, $d \in R^n$, $u \in R^p$, $y_A \in R^q$. For the control of aircraft, the states are given by the vector x_A and may include the angle of attack, the pitch rate, the angle of sideslip, the roll rate, and the yaw rate ($n=5$). The output vector y_A may contain the pitch rate, the roll rate, and the yaw rate ($q=3$). The control input vector u consists of the commanded actuator positions. In a conventional aircraft, these commands are the deflections of two elevators, two ailerons, and the rudder ($p=5$). The disturbance vector d represents the forces and moments that the control surfaces must cancel in order to trim the aircraft (*i.e.*, to create an equilibrium of the dynamical system).

For the purpose of example, consider a simple model reference control law. The method relies on a reference model that represents the desired dynamics of the closed-loop system

$$\dot{y}_M = A_M y_M + B_M r_M \tag{2}$$

where r_M is a reference input vector (the pilot commands) and y_M represents the desired output of the system. Since the derivative of y is given by

$$\dot{y}_A = CA_A x_A + CBu + Cd \tag{3}$$

the objective may be achieved by setting

$$CBu = -CA_A x_A - Cd + A_M y_A + B_M r_M \equiv a_d \tag{4}$$

where a_d represents the desired vector to be matched by CBu. If y is a vector composed of the incremental rotational rates (as is typically the case), a_d represents the desired incremental rotational accelerations, and u represents the incremental surface deflections.

Obtaining u from a_d requires that one solve a system of linear equations with more unknowns than equations. Solving such a system is easy, but the difficulty in control allocation is that the vector u is constrained. The limits generally have the form

$$u_{\min,i} \le u_i \le u_{\max,i} \qquad \text{for } i = 1,\ldots,p \tag{5}$$

where p is the number of surfaces. In vector form, Eq. 5 is written as $u_{\min} \le u \le u_{\max}$. There may be additional constraints due to the maximum rate of deflection of the actuators. We refer to the problem of finding a vector u that is the "best" possible solution of Eq. 4 within the constraints Eq. 5 as the *control allocation problem*.

Given the constraints, the control allocation problem may be such that:

- many solutions exist,
- only one solution exists,
- no exact solution exists.

One is naturally drawn to finding solutions that minimize the error CBu-a_d. Indeed, providing all the control authority available may make the difference between a maneuver being achievable or not, and between an unusual condition being recoverable from or not. However, the question also arises as to which solution is the most desirable when many solutions exist. Therefore, optimal control allocation typically consists both of *error minimization* and *control optimization*. As we will discuss in this paper, the objective of load minimization, or at least load limiting, may also become part of the control allocation problem.

B. Formulations of optimal control allocation

The fundamental control allocation problem can be formulated as the following error minimization objective.

Error minimization: given a matrix CB, find a vector u such that

$$J = \|CBu - a_d\| \tag{6}$$

is minimized, subject to $u_{\min} \le u \le u_{\max}$.

The problem is solved exactly if $J=0$. However, regardless of whether an exact solution exists, the following control minimization problem may be considered as well.

Control minimization: given a matrix CB, a vector u_p, and a solution vector u_1 such that $u_{\min} \le u_1 \le u_{\max}$, find a vector u such that

$$J = \left\| u - u_p \right\| \tag{7}$$

is minimized, subject to

$$(CB)u = (CB)u_1 \tag{8}$$

and $u_{\min} \le u \le u_{\max}$.

The control minimization problem is a secondary optimization objective to be satisfied if the solution of the primary objective, given by u_1, not unique. The vector u_p represents some preferred position of the actuators (*e.g.*, one that yields zero deflections of the surfaces). After a solution yielding minimum error is obtained, the solution with minimum deviation from the preferred position is picked among all equivalent solutions. For both problems, weighting of the elements of the vectors may be inserted in the norms, either to prioritize the axes or to prioritize the actuators.

The norm used in the optimization criteria is a design choice that has more consequences than might be expected. The l_1 norm of a vector x is the sum of the absolute values of the elements of the vector

$$\|x\|_1 = \sum_{i=1}^{n} |x_i| \tag{9}$$

while the l_2 norm is the usual Euclidean norm

$$\|x\|_2 = \sqrt{\sum_{i=1}^{n} |x_i|^2} \tag{10}$$

and the l_∞ norm is the sup norm

$$\|x\|_\infty = \max_i |x_i| \tag{11}$$

A possible implementation of optimization for control allocation consists in the sequential minimization of the error vector and of the control vector. Specifically, the error is minimized first, and then the control vector is minimized among all equivalent solutions. In Ref. 11, the control minimization problem was solved only when the solution of the primary error minimization problem was $J=0$. However, it should be noted that, unless the matrix CB satisfies specific conditions (any $q \times q$ submatrix of CB must be nonsingular), the solution is not necessarily unique, even if the desired vector a_d is not feasible. Given this fact, mixed optimization makes sense, and has several advantages over sequential optimization.

Mixed optimization: Given a matrix CB and a vector u_p, find a vector u such that

$$J = \left\| CBu - a_d \right\| + \varepsilon \left\| u - u_p \right\| \tag{12}$$

is minimized, subject to $u_{\min} \le u \le u_{\max}$.

The mixed optimization problem combines the error and control minimization problems into a single problem through the use of a small parameter ε. If the parameter ε is small, priority is given to error minimization over

control minimization, as is normally desired. Often, the combined problem may be solved faster, and with better numerical properties, than when the error and control minimization problems are solved sequentially[8].

C. Implementation of optimal control allocation algorithms

Computational resources available on modern aircraft make the use of optimal control allocation algorithms feasible in real-time. An efficient algorithm to solve the mixed optimization problem given in Eq. 12 with the l_1 norm on the criterion was formulated by Bodson using linear programming approaches, providing guaranteed convergence to a solution in an acceptable period of time[8]. Timing data showed that solutions of the problem could comfortably be performed in real-time, even for large numbers of actuators, and that the optimal solution improved performance significantly over simpler, approximate methods. The algorithm was based on the revised simplex method[19] with additional refinements, such as anticycling, as described in detail in Ref. 8.

Harkegård proposed an elegant solution of the optimal control allocation problem using the l_2 norm and the theory of active sets[15]. The algorithm was very similar to the simplex algorithm used for l_1 optimization, and had the same advantage of completing in finite time and with a small number of iterations.

Reference 17 describes and compares several new algorithms that use different combinations of norms on the optimization criteria. A particularly promising algorithm uses the l_1 norm for error minimization and the l_∞ norm for control minimization, with both criteria combined in a single, mixed optimization criterion. The min-max criterion results in a type of resource-balancing, where the resources are the control surface deflections and the algorithm balances those resources to achieve the desired command. A small modification to the approach used in Ref. 8 for mixed l_1 optimization yields the desired linear program.

A further modification to the algorithm using the l_∞ norm for control minimization yields the solution of a new problem where the actuator deflections are weighted in the computation of the l_∞ norm as per unit values, where a unit is the maximum deflection of the actuator[17]. In this algorithm, minimization of the control effort translates into minimization of the maximum actuator deflection as a percentage of its range of motion. Advantages of the resource-balancing feature were shown to include a greater resilience to actuator failures and to nonlinear effectiveness for large actuator deflections.

III. Control Allocation with Structural Load Constraints and Load Feedback

Most optimal control allocation algorithms find an optimal solution to the control allocation problem within the constraints of the control surface position and possibly rate limits. However, these constraints are not sufficient to ensure that the structural load limits of the aircraft will not be exceeded by the commanded control surface deflections. The bending and torsion moments at the wing root are examples of loads on the aircraft that need to be monitored. In this section, we formulate the load constraints at discrete critical points on the aircraft as

$$\left\| M + Tu \right\| \le L_{max} \tag{13}$$

where $\boldsymbol{M}$ is a vector of the current measured or estimated loads at the critical points, $\boldsymbol{T}$ is a matrix that converts the effect of incremental surface deflections into incremental structural loads, and $\boldsymbol{L}_{max}$ is a vector of maximum allowable structural loads at the critical points. The loads that need to be limited are a function of the aircraft being considered, often with an emphasis on torsion and bending moments and shear forces. Generally, the load limits are determined through detailed studies, including ground and flight tests. This paper will not address the selection of the location or the number of load points to be considered for a given problem. For the purpose of developing a representative example, we choose load points along the aircraft wing, horizontal tail, and vertical tail.

We assume that the $\boldsymbol{T}$ matrix, which is computed from the states of the aircraft at the current time, gives a linear approximation of the incremental structural loads arising from commanded surface deflections. The incremental loads matrix is formed by perturbing each control surface deflection from its current position at the current aircraft state. The perturbation yields the change in aerodynamic lift and rolling moments due to a one-degree change in surface deflection. It is assumed that the lift due to the wings is elliptically distributed along the span of each wing. It is also assumed that the control effectiveness of each surface is proportional to the lift generated by that control surface. The resulting lift and moment components are used in conjunction with a structural model of the aircraft to determine moments at critical points on the aircraft. Superposition of the control surface effects in terms of lift, moments, and structural loads is assumed in order to obtain a reasonable, but tractable solution in real-time.

The structural load limits can be implemented as an additional constraint as given in Eq. 13. Additionally, the control allocation cost function can include a term to minimize the loads at the critical points, as given below

$$J = \left\| CBu - a_d \right\| + \varepsilon \left\| u - u_p \right\| + \gamma \left\| M + Tu \right\| \tag{14}$$

The l_∞ norm could be used on the load minimization criterion in Eq. 14 in an implementation that is similar to its use on the control minimization described in Section II (c). Also, the critical load points could be weighted in the computation of the l_∞ norm as per unit values, where a unit is the maximum load limit of the critical point. Using this approach, solutions could be obtained that more evenly distribute loads at the critical points.

IV. Proof of Concept Simulation Architecture

In this section we describe the proof of concept simulation implemented to demonstrate the proposed framework assuming static loads, an elliptical lift distribution, and a limited number of critical load points. An earlier study[18] had a similar architecture, but only modeled the aircraft wings and used the l_1 norm. Use of the most effective surfaces is a recognized consequence of using the l_1 norm in control allocation. This effect was observed in the previous study, and it was seen to be a limitation.

A. Aircraft configuration and aerodynamic model

A full nonlinear simulation of a class of full-scale generic transport aircraft is used for the proof of concept study of the proposed framework. The simulation uses a dynamically scaled representative transport model that is derived from a model of NASA's AirSTAR testbed. The AirSTAR testbed is being developed as part of NASA's Aviation Safety Program to investigate dynamics modeling and control of large transport vehicles in upset conditions[20]. The AirSTAR unmanned aerial vehicle (UAV) is a 5.5% dynamically scaled aircraft based on wind tunnel and flight test data[21]. The simulation used in this paper is a full-scale model that was derived from the subscale model by incorporating Reynolds adjusted aero tables, actuator models appropriate for a full-scale aircraft, and a model of NASA Glenn's Simp2 engine which is a simplified version of C-MAPSS40k.

The simulation created for this study represents a conventional modern midsize commercial passenger configuration. The aircraft has right and left inboard and outboard elevons, three ailerons on each wing, and upper and lower rudders for use by the control allocator to achieve the desired roll, pitch, and yaw moments commanded by the flight control system. A stabilizer is used for trimming the aircraft.

For the proof of concept study, seventeen critical points on the aircraft were monitored for bending moments. Each wing had critical points located at the wing root and at locations inboard of each aileron. The bending moments were monitored at locations inboard of each elevon on the horizontal tail and at the root. The vertical tail had three monitored points at the root and upper and lower rudders. The load limits were set to $\pm 5.3 \times 10^6$ for all of the critical points. These values were chosen for simplicity and to ensure that the baseline maneuver would not cause any load limiting.

B. Static structural model

A finite element analysis (FEA) model is developed and integrated into the simulation to estimate static structural loads on the aircraft due to lift and roll moments and to compute the incremental loads created by surface deflections. For the proof of concept study, bending moments on the wing, tail and rudder are monitored. The finite element method is employed for its ability to calculate internal loads for potentially complex load distributions and geometries at different locations on-the-fly. The basic FEA model requires a small number of matrix multiplications for static loads analysis. Furthermore, the finite element method provides an efficient framework for adding additional monitored points. In implementing this approach, we hope to determine whether the required computations are fast enough and accurate enough for flight controllers in both real-time simulations and actual flight.

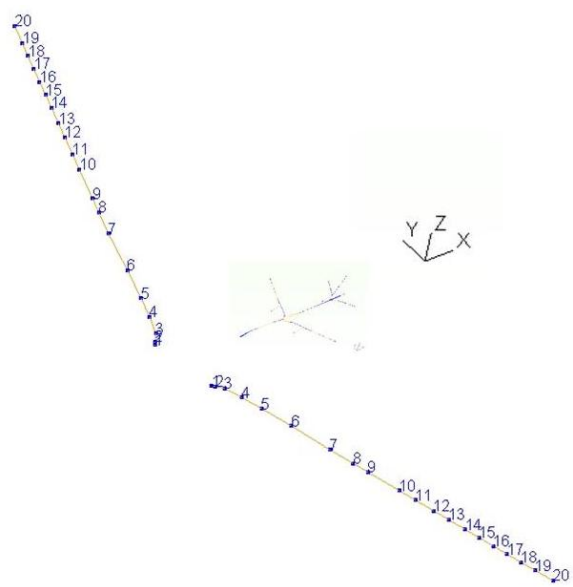

Fig. 1. Finite element beam model for left and right wings.

The FEA modeling is simplified to beam modeling, based on mass and stiffness approximations for a representative full-scale generic civil transport model. The model includes two beam meshes for representing the left and right wings independently, and two beam meshes for the horizontal tails and one beam mesh for the vertical tail. Figure 1 shows the two wing meshes with the node numbers. Each wing mesh has 20 nodes and 19 beams. The wings are modeled as cantilever beams with the fixed ends at the wing roots. All degrees of freedom for node 1 are fixed for both meshes. The global coordinates of the finite element model are attached to the aircraft, with the origin at the nose, positive *X*-axis pointing toward the tail, and positive *Z*-axis pointing up. We use a simplified approximation of the wing as hollow aluminum shells having the wing outer mold line of the representative aircraft and a constant thickness of five inches. Beam cross section properties are calculated using this hollow shell wing geometry. Figure 2 shows nodes of the right wing beam mesh running through centroids of the wing cross sections.

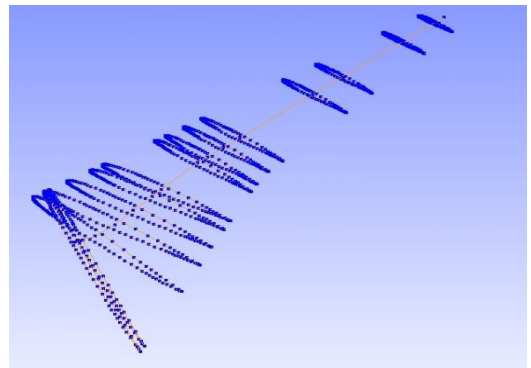

Fig. 2. Beam nodes located at centroids of wing cross sections.

The C^0 approach as described in Ref. 23 is used for the beam modeling. There are three translation and three rotation degrees of freedom per node. A linear shape function with one-point reduced integration is used for the axial, transverse shear, torsion and transverse bending components. The "residual bending flexibility" technique[23] is also applied to the shear term to improve the accuracy of the two-node, one-point quadrature beam element. The displacement solution for the static problem is given by

$$d = K^{-1}F \tag{15}$$

where $\boldsymbol{d}$ is a vector containing the displacement solutions, $\boldsymbol{K}$ is the stiffness matrix of the wing structure, and $\boldsymbol{F}$ is a vector of external loads applied to the structure. All terms in Eq. 15 are calculated in the global coordinate system. The internal moment about local beam direction 2, $\boldsymbol{M_2}$, is the bending moment used as the measured load at the critical points passed to the control allocator in the simulation. The calculation for the internal moment for the beams is given by

$$M_2 = EI_{22}k_{22} \tag{16}$$

where $\boldsymbol{E}$ is Young's modulus, $\boldsymbol{I_{22}}$ is the second moment of inertia about the local 2 beam axis, and $\boldsymbol{k_{22}}$ is the curvature about the local 2 beam axis, which is calculated from the displacement solutions and the beam finite element shape function.

The structural modeling and analysis used for this study assumes static conditions and considers external loads on the wing due to aerodynamic lift forces and roll moments. The lift distribution on each wing is assumed to be elliptical, with each wing carrying half of the lift due to the wings. Figure 3 shows the normalized lift per length distribution for each wing. The external loads arising from the roll moment on the aircraft wing are assumed to be from concentrated forces applied in the aircraft *Z* direction at the ailerons. These forces are applied to nodes 15, 17, and 19, located at the center of the three ailerons on each wing. The *Z* direction force acting on each aileron is assumed to be proportional to the aileron deflections. The horizontal and vertical tails are treated in a similar manner.

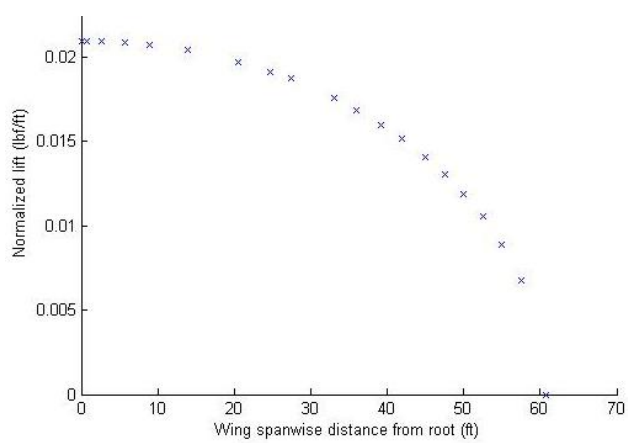

Fig. 3. Normalized lift load on each wing (lbf/ft).

To minimize computation time, $\boldsymbol{K}$ is calculated and inverted in a pre-processing step prior to running the simulation. The normalized lift force of 1lbf with the elliptical distribution shown in fig. 3 is also calculated in the pre-processing step. The total force $\boldsymbol{F}$ on each wing is computed as the sum of (*i*) the wing's lift using

the elliptical lift force distribution and (*ii*) any roll forces at the aileron nodes (15, 17, 19). The loads are calculated in a similar manner for the aircraft tail.

The simulation uses the calculated forces to compute the displacements as given by Eq. 15. The bending moments at the critical points are then derived from the displacements and the structural model. The aileron critical points are at the aileron inboard edges, nodes 14, 16, and 18. These estimated bending moments are used as the simulated current load measurements at the critical points.

The incremental load matrix $\boldsymbol{T}$ represents the change in internal loads on the wing or tail due to a change in the surface deflection from the current position. It is computed by determining the change in lift and moment forces due to a one-degree change in control surface deflection from the current surface position.

C. Stability and control augmentation system with optimal control allocation

The stability and augmentation system for the simulation uses a dynamic inversion controller with a second order reference model. The simulation has multiple surfaces that control multiple axes. The control allocator is able to use these surfaces to achieve the desired roll, pitch, and yaw moments commanded by the flight control system. The allocator has inputs for measured load $\boldsymbol{M}$, the incremental load matrix $\boldsymbol{T}$ for predicting the control surface contribution to the load at the critical points, a preferred position $\boldsymbol{u_p}$, surface position limits, and load limits. The load limits are incorporated as a constraint on the cost function. Since this paper is looking at the feasibility of the framework, we are only considering the load constraint on the bending moments at the 17 critical points along the wings and tail. The control allocation problem solved in this simulation is to find the vector u such that

$$J = \left\| CBu - a_d \right\|_1 + \varepsilon \left\| u - u_p \right\|_\infty \tag{19}$$

is minimized, subject to $u_{\min} \le u \le u_{\max}$ and $\left\| M + Tu \right\| \le L_{\max}$. The above criterion and constraints are converted to a linear program and solved using the revised simplex algorithm described in Section II (c), which was modified to include the load constraints. The control allocator does not have actuator rate limits as a constraint, but the actuators modeled in the simulation rate limit their commands. The control minimization criterion was weighted in the control allocator by setting $\varepsilon=10^{-4}$. Scaling of some of the inputs to the control allocator was necessary to achieve good numerical properties for the algorithm. The parameters $\boldsymbol{CB}$ and $\boldsymbol{a}_d$ were scaled by a factor of 10^{-3} and the structural load parameters $\boldsymbol{M}$, $\boldsymbol{T}$, and $\boldsymbol{L}_{\max}$ were scaled by a factor of 10^{-4}.

V. Simulation Results

Simulations with the architecture described in Section IV were tested for representative scenarios that could occur in a damaged aircraft. We chose a roll doublet for the proof of concept criterion. The roll doublet can be performed under normal operating conditions without causing excessive maneuver loads that exceed the default load limits. The simulations were run after the aircraft was trimmed at Mach 0.70 and 30,000 feet. A baseline case with default load constraints was used for comparison, see fig. 4.

The first test case was designed to emulate a fault that required reducing loads at a particular location on the aircraft. The monitored point to the left of the outboard aileron on the right wing (node 18) was chosen for case 1. The bending moment load limit for the monitored point was reduced to $5.5\text{x}10^5$ ft-lb. Figure 4 shows the commanded rates and the aircraft response to the doublet command. The bending loads experienced at the monitored point near the right wing's outboard aileron are shown

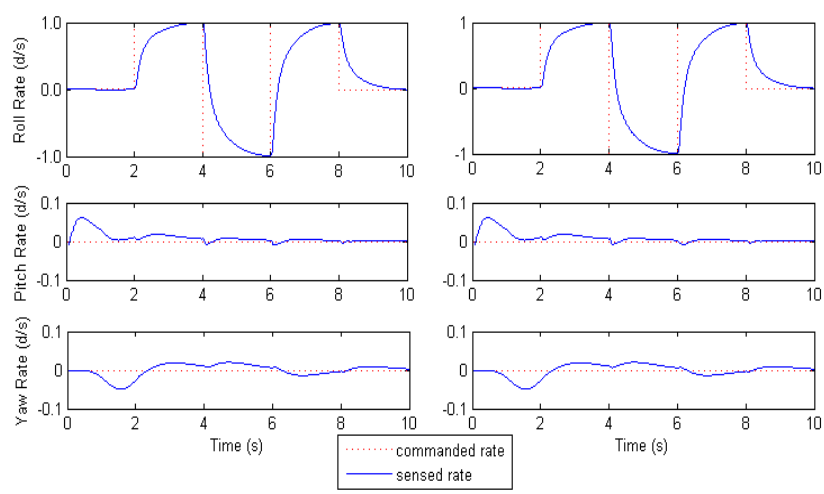

Fig. 4. Commanded and sensed rates with baseline load limits (left column) and with reduced load limits (right column).

in fig. 5. The left-hand plot is the baseline case and the right-hand plot is case 1, where the monitored location has a reduced load limit. The control allocator uses a different combination of control surfaces to achieve the desired command without exceeding the load limits.

The deflections of the ailerons and elevons for the roll doublet for the baseline case and case 1 are shown in figs. 6 and 7, respectively. The change in surface deflections between the baseline case and case 1 is relatively small, but one can see that the inboard ailerons deflect further when the load limit is reduced. The ailerons inboard of the monitored point only contribute indirectly to the measured load by creating the desired roll moment. The elevons also show slightly larger anti-symmetric deflections than those seen in the baseline case. The relatively small change in the loads is due in to the fact that the maneuver contributes more to the loads than the actual surface deflection of the outboard aileron.

A second test case illustrates a situation where the health management system detects an actuator fault that might lead to a stuck control surface, and so the surface deflection is limited. This is accomplished by setting the maximum and minimum surface deflection limits to ±0.01 degree for the outboard aileron on the left wing. The right-hand plot in fig. 8 shows the resulting surface deflections for the aircraft wing compared to the baseline plot on the left-hand side. The aircraft is able to achieve the desired rates with results comparable to fig. 4. Note that the outboard aileron on the left wing does not move when the position limits are changed.

The second test case demonstrates the versatility of the framework incorporating optimal control allocation. As long as the commands coming from the flight control system are achievable with the available control power, the stability of the system will not be affected. An important consideration when limiting control surface authority, by limiting surface deflection, is whether the aircraft will have enough authority in all three axes to safely accomplish its mission. When using this framework for either of the two cases described in this situation, the system would need to smoothly transition to the new position limits or load limits so that the surfaces do not behave erratically.

Several other scenarios were tested in which the load limits and position limits were changed. Results were comparable to those reported here. The allocator was able to handle multiple position constraints that still enabled the desired commands to be achieved. Studies of the affects of weights on certain control surfaces or critical points showed

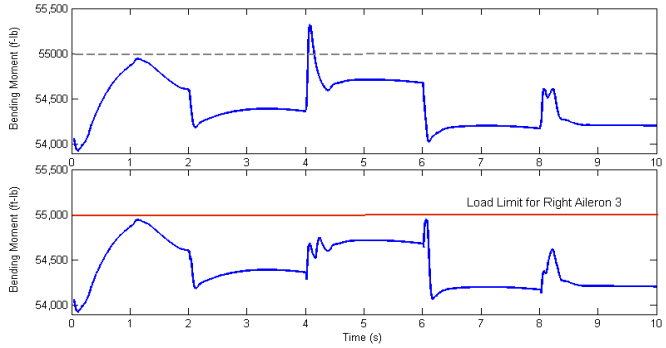

Fig. 5. Bending moment (ft-lb) at right outboard aileron 3 critical point, baseline case (top) and case 1 (bottom).

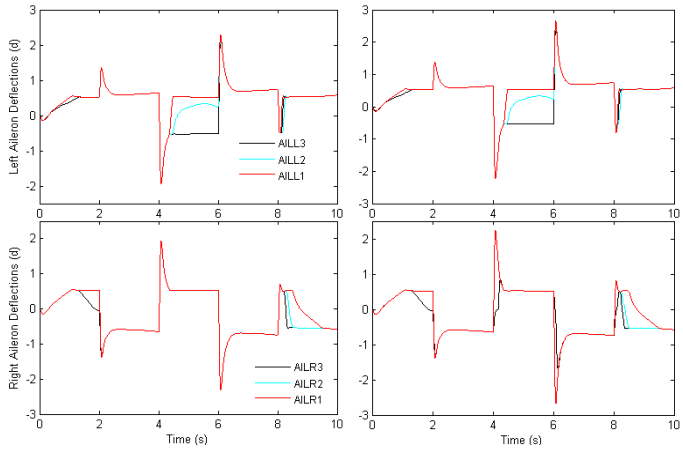

Fig. 6. Aileron deflections in degrees for baseline (left) and case 1 (right).

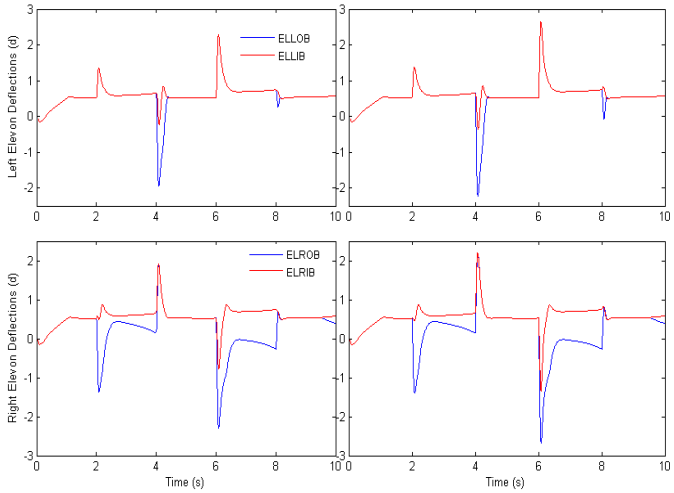

Fig. 7. Elevon surface deflections in degrees for baseline (left) and case 1 (right).

promise for shaping the control allocator's solutions. Further studies of these algorithms will be necessary to determine their suitability for flight. This is beyond the scope of this paper which was intended to show proof of concept and demonstrate how optimal control allocation could be used with system health management or PHM.

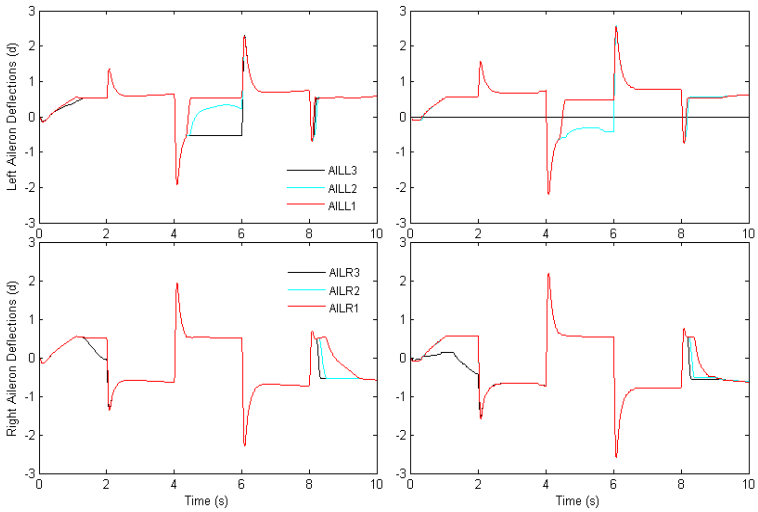

Fig. 8. Aileron surface deflections in degrees. Left column is baseline case. Right column is case 2 (normal limits except outboard left aileron (AILL3) has limits ±0.05 d).

VI. Conclusions & Future Work

A flight control framework is proposed and demonstrated in simulation, using load constraints and real-time load feedback in conjunction with optimal control allocation. The framework was used to demonstrate how faults can be accommodated to perhaps avoid further damage and increase safety.

Optimal control allocation using the l_∞ norm on the control criterion was demonstrated to command surface deflections to achieve desired moments while remaining within the defined structural load limits of the aircraft and position limits of the control effectors. The algorithm with the l_∞ norm produced more even distribution of the control resources, in the form of control surface deflections. The framework was demonstrated on two cases of faults that might occur during flight which the health management system would need to address to improve safety. The flight control system responded as expected to changes commanded by the health management system.

This study reveals many interesting problems for future investigation. The use of weights on the surfaces and critical load points in the control allocation cost function needs further investigation. Adding the ability to minimize one or more monitored load points will be explored as a means to reduce loads at monitored points without needing to specify a precise limit. Including load minimization allows the algorithm more flexibility when finding a solution. However, adding another criterion to the cost function complicates the behavior of the solution.

Robustness of the load model and the incremental loads matrix need to be examined in much more detail. Many challenges will undoubtedly arise when integrating information from the sensed loads on the aircraft with the structural model. A step towards addressing this issue can be partially examined by adding sensor noise, bias, and other errors to the measured loads in the simulation. Future work will be done to add structural dynamics to the model and include additional load paths and torsion.

Studies of the integrated flight control system to determine the robustness and sensitivity to errors in the load measurements and incremental loads matrix will be essential before transitioning to a system with load measurements coming from sensors. At this time, the computation time for this simulation is reasonable. However, as the system becomes more complex, methods to increase the computation speed may become necessary. One area of investigation is whether some load paths could be ignored at certain parts of the flight envelope. Another important question is how often the load measurements and the incremental load matrix need to be and can be updated.

Future work will investigate the extension of the control system framework presented in this paper to gust load alleviation. Sensors, modeling, or a combination of both will provide the current load at critical points while a matrix similar to the $\boldsymbol{T}$ matrix will give the incremental load per incremental gust. Given an estimate of an upcoming gust, its load can be predicted and an optimal control allocator can use appropriate surfaces to counteract the predicted load.

There are many open areas of research in the use of real-time load feedback in flight control systems to improve safety and performance. Future aircraft will likely employ some sort of real-time load feedback as materials, sensors, computation power, and aircraft configurations evolve.

Acknowledgments

Special thanks to Dr. Kai Goebel of NASA Ames Research Center for his support and motivation for this work.

References

[1]"Fundamental Aeronautics Research Directorate", National Aeronautics and Space Administration, June 2011, URL: http://www.aeronautics.nasa.gov

[2]Doebling, S.W., Farrar, C.R., Prime, M.B., Shevitz, D.W., "Damage identification and health monitoring of structural and mechanical systems from changes in their vibration characteristics: A literature review," Technical Report LA--13070-MS, Los Alamos National Lab., NM, May 1996.

[3]Y. M. Zhang and J. Jiang, "Bibliographical Review on Reconfigurable Fault-Tolerant Control Systems," in Proc. of the *5th IFAC Symposium on Fault Detection, Supervision and Safety of Technical Processes*, Washington, D.C., USA, June 9-11, 2003, pp. 265-276.

[4]D. Shore and M. Bodson, "Flight Testing of a Reconfigurable Control System on an Unmanned Aircraft," *AIAA Journal of Guidance, Control, and Dynamics*, vol. 28, no. 4, pp. 696-707, 2005.

[5]J. S. Litt, K. J. Parker, and S. Chatterjee, "Adaptive Gas Turbine Engine Control for Deterioration Compensation due to Aging," Technical Report TM 2003-212607, NASA Glenn, Lewis, OH. 2003.

[6] Liang Tang, Gregory J. Kacprzynski, Kai Goebel, Abhinav Saxena, Bhaskar Saha, and George Vachtsevanos, "Prognostics-enhanced Automated Contingency Management for Advanced Autonomous Systems," *International Conference on Prognostics and Health Management*, Denver, CO, October 6, 2008 – October 9, 2008.

[7] Farrar, Charles R. and Lieven, Nick A.J., "Damage prognosis: the future of structural health monitoring," *Phil. Trans. R. Soc. A*, 365(1851), pp. 623-632.

[8]Bodson, M., "Evaluation of Optimization Methods for Control Allocation," *AIAA Journal of Guidance, Control, and Dynamics*, vol. 25, no. 4, pp.703-711, 2002.

[9]Durham, W. "Constrained Control Allocation," *Journal of Guidance, Control, and Dynamics*, vol. 16, no. 4, 1993, pp. 717-725.

[10]Enns, D., "Control Allocation Approaches," *AIAA Guidance, Navigation and Control Conference and Exhibit*, AIAA, Boston, MA, August 1998, AIAA-1998-4109.

[11]Buffington, J. "Modular Control Law Design for the Innovative Control Effectors (ICE) Tailless Fighter Aircraft Configuration 101-3," Report AFRL-VA-WP-TR-1999-3057, Air Force Research Laboratory, Wright-Patterson AFB OH 45433-7542, 1999.

[12]Burken, JJ, Lu, P., Wu, Z. & Bahm, C., "Two Reconfigurable Flight-Control Design Methods: Robust Servomechanism and Control Allocation," *Journal of Guidance, Control, and Dynamics*, vol. 24, no. 3, 2001, pp. 482-493.

[13]Petersen, J. & Bodson, M., "Interior-Point Algorithms for Control Allocation," *Journal of Guidance, Control, and Dynamics*, vol. 28, no. 3, 2005, pp. 471-480.

[14]Petersen, J. & Bodson, M., "Constrained Quadratic Programming Techniques for Control Allocation," *IEEE Trans. on Control Systems Technology*, vol. 14, no. 1, January 2006, pp. 91-98.

[15]Härkegård, O., "Efficient Active Set Algorithms for Solving Constrained Least Squares Problems in Aircraft Control Allocation," *41st IEEE Conference on Decision and Control*, Vol. 2, pp. 1295-1300.

[16]Oppenheimer, M. W. & Doman, D. B., "A Method for Including Control Effector Interactions in the Control Allocation Problem," report AFRL-VA-WP-TP-2007-309, Air Force Research Laboratory, Wright-Patterson AFB, OH 45433-7542, 2007.

[17]Bodson, M. & Frost, S., "Load Balancing in Control Allocation", *Journal Guidance, Control and Dynamics*, Vol. 34, No. 2, pp. 380-387, March–April 2011.

[18]Frost, S.A., Taylor, B.R. Jutte, C.V, Burken, J.J., Trinh, K.V., & Bodson, M., "A Framework for Optimal Control Allocation with Structural Load Constraints," *Proceedings AIAA Atmospheric Flight Mechanics Conference*, AIAA, Toronto, ON, Canada, August 2010.

[19]Luenberger, D., *Introduction to Linear and Nonlinear Programming*, Addison-Wesley, Reading, MA 1984, pp. 80.

[20]Jordan, T.L., Foster, J.V., Bailey, R.M., & Belcastro, C.M., "AirSTAR: A UAV Platform for Flight Dynamics and Control System Testing", AIAA 2006-3307, *25th AIAA Aerodynamic Measurement Technology and Ground Testing Conference*, AIAA, San Francisco, CA, 2006.

[21]Jordan, T.L., Langford, W.M., and Hill, J.S., "Airborne Subscale Transport Aircraft Research Testbed, Aircraft Model Development", AIAA 2005-6432, *AIAA Guidance, Navigation, and Control Conference*, AIAA, Washington, DC, 2005.

[22]"Quadratic Programming Control Allocation Toolbox (QCAT)," Matlab® Central, July 2011, URL: http://www.mathworks.com/matlabcentral/fileexchange/loadFile.do?objectId=4609&objectType=file

[23]Hughes, Thomas J.R., *The Finite Element Method-Linear Static and Dynamic Finite Element Analysis*, Springer-Verlag, New York, 1983, Chapter 5.